Assessment of Debonding and Particulate Fracture Occurrences in Circular Silicon Nitride Particulate/AA5050 Alloy Metal Matrix Composites

A. Chennakesava Reddy

[2]Assistant Professor, Department of Mechanical Engineering, MJ College of Engineering and Technology, Hyderabad, India
dr_acreddy@yahoo.com

Abstract: *Square array unit cell/circular particulate RVE models are employed to asses debonding and particulate fracture occurence using two-dimensional finite element methods under plane strain conditions. The particulate metal matrix composites are silicon nitride/AA5050 alloy at different volume fractions of silicon nitride. There is strong likelihood of debonding at the particle-matrix interface.*

Keywords: AA5050*, silicon nitride, circular particle, RVE model, finite element analysis, interfacial tractions, debonding.*

1. INTRODUCTION

Effectiveness of strengthening with metal matrix composites depends largely on the reinforcement material and the type of the matrix material to be strengthened [1, 2]. In a strengthening mechanism, the strengthening reinforcement material is generally expected to have a higher stiffness compared to the matrix material being strengthened [3, 4]. Debonding in strengthened particulate metal matrix composites takes place in regions of high stress concentrations, which are often associated with material discontinuities, shape of reinforcement particulates and with the presence of cracks or voids [5, 6]. Propagation path of debonding initiated from stress concentrations is dependent on the elastic and strength properties of matrix and reinforcement materials as well as their interface fracture properties [7, 8, 9]. Various particulate and matrix combinations have been tested for micromechanical behavior. The material combinations include boron carbide/AA1100 [10], boron carbide/AA3003 [11], boron carbide/AA4015 [12], boron carbide/AA5050 [13], boron carbide/AA8090 [14], titanium boride/AA3003 [15], titanium boride/AA5050 [16], titanium boride/AA7020 [17], titanium boride/AA8090 [18], silicon nitride/AA1100 [19], silicon nitride/AA2024 [20], silicon nitride/AA3003 [21] and silicon nitride/AA4015 [22].

The present research aims to assess the particle fracture or the debonding occurrence of silicon nitride/AA5050 alloy particulate metal matrix composites. Finite element method is used to construct and analyze the different (representative volume elements (RVEs) models of periodic circular particulates in a square array distribution.

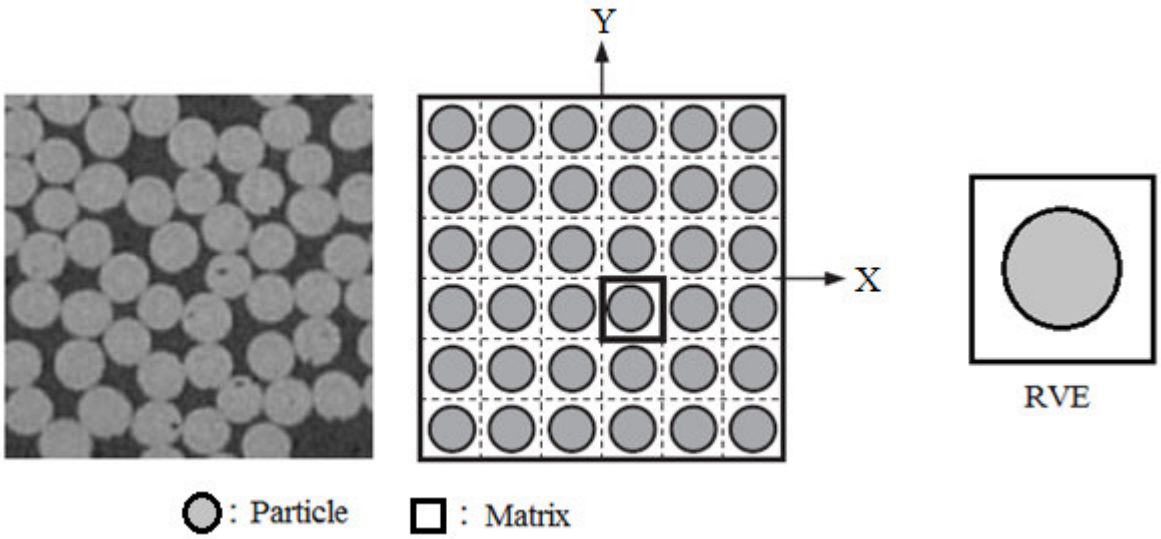

Figure 1: The RVE model: (a) particle distribution and (b) RVE scheme.

2. MATERIALS AND METHODS

The volume fractions of silicon nitride particle reinforcement were 10%, 20%, and 30% in the matrix AA5050 alloy. The periodic model for the representative volume element (RVE) scheme is shown in figure 1. The perfect adhesion was assumed between titanium boride particle and AA5050 alloy matrix. PLANE183 element was used for the matrix and the nanoparticle. The interface between particle and matrix was modeled using CONTACT -172 element.

The shear lag model [1] has been used to describe the build up and transfer of particle stress, σ_p from the point where the particle enters the matrix to some point along the particle axis where the tensile stress has decayed to zero. Failure of the particle/matrix interface occurs when the interfacial shear strength, τmax, is reached.
The shear lag distribution of strain, along a fully bonded particle can be described by [1]

$$e_{app} = e_p \frac{sibh[n(L_{e-x/r})]}{sinH(ns)} \quad (1)$$

where e_{app} is the strain acting on the particle outside the matrix, e_p is the particle strain at a distance x inside the matrix, L_e is the embedded length, r is the particle radius and s is the particle aspect ratio (L_e/r). The *n* parameter used in this paper is based on the parameter derived by Nairin [2]:

$$n^2 = \frac{2}{E_p E_m}\left[\frac{E_p V_p + E_m V_m}{V_m/(4G_p)+1/(2G_m)\left((1/V_m)\ln(1/V_p)-1-(V_m/2)\right)}\right] \quad (2)$$

where E_p and G_P ate the particle elastic and shear moduli, E_m and G_m are the elastic and shear moduli of the matrix. V_p is the particle volume fraction and V_m is the volume fraction of matrix. The corresponding interfacial stress, τ at a distance x along the interface, is given by

$$\tau = \frac{n}{2} E_p e_{app} \frac{\cosh[n(L_e-x)/r]}{\sinh[ns]} \quad (3)$$

Is a maximum at the crack plane ($x = 0$). Since both the interfacial shear stress and the stress acting on the particle, are a maximum at the crack-plane then failure should be expected to initiate from this point. When $x = 0$, the Eq. (3) becomes:

$$\tau = \frac{n}{2} E_p e_p \quad (4)$$

If the particle deforms in an elastic manner (according to Hooke's law) then,

$$\tau = \frac{n}{2} \sigma_p \quad (5)$$

where σ_p is the particle stress. If particle fracture occurs when the stress in the particle reaches its ultimate tensile strength, $\sigma_{p,uts}$, then setting the boundary condition at

$$\sigma_p = \sigma_{p,\,uts} \quad (6)$$

and substituting into Eq.(5) gives a relationship between the strength of the particle and the interfacial shear stress such that if

$$\sigma_{P,uts} < \frac{2\tau}{n} \quad (7)$$

Then the particle will fracture. Similarly if interfacial debonding/yielding is considered to occur when the interfacial shear stress reaches its shear strength

$$\tau = \tau_{max} \quad (8)$$

Then by substituting Eq. (8) into Eq.(5) a boundary condition for particle/matrix interfacial fracture can be established whereby,

$$\tau_{max} < \frac{n\sigma_p}{2} \quad (9)$$

This approach suggests that the outcome of a matrix crack impinging on an embedded particle depends on the balance between the particle strength and the shear strength of the interface.

Surface tractions, or stresses acting on an internal datum plane, are typically decomposed into three mutually orthogonal components. One component is normal to the surface and represents direct stress. The other two components are tangential to the surface and represent shear stresses. The definition of the tractions in terms of stresses is shown in figure 2.

A linear stress–strain relation at the macro level can be formulated as follows:

$$\bar{\sigma} = \overline{C}\,\bar{\varepsilon} \quad (10)$$

where $\bar{\sigma}$ is macro stress, and $\bar{\varepsilon}$ represents macro total strain and $\overline{C}$ and is macro stiffness matrix.

For plane strain conditions, the macro stress- macro strain relation [3-12] is as follows:

$$\begin{Bmatrix} \overline{\sigma_x} \\ \overline{\sigma_y} \\ \overline{\tau_{xy}} \end{Bmatrix} = \begin{bmatrix} \overline{C_{11}} & \overline{C_{12}} & 0 \\ \overline{C_{21}} & \overline{C_{22}} & 0 \\ 0 & 0 & \overline{C_{33}} \end{bmatrix} \times \begin{Bmatrix} \overline{\varepsilon_x} \\ \overline{\varepsilon_y} \\ \overline{\gamma_{xy}} \end{Bmatrix} \quad (11)$$

The interfacial tractions can be obtained by transforming the micro stresses at the interface as given in Eq. (3):

$$t = \begin{Bmatrix} t_z \\ t_n \\ t_t \end{Bmatrix} = T\sigma \qquad (12)$$

where, $T = \begin{bmatrix} 0 & 0 & 0 \\ cos^2\theta & sin^2\theta & 2sin\theta cos\theta \\ -sin\theta cos\theta & sin\theta cos\theta & cos^2\theta - sin^2\theta \end{bmatrix}$

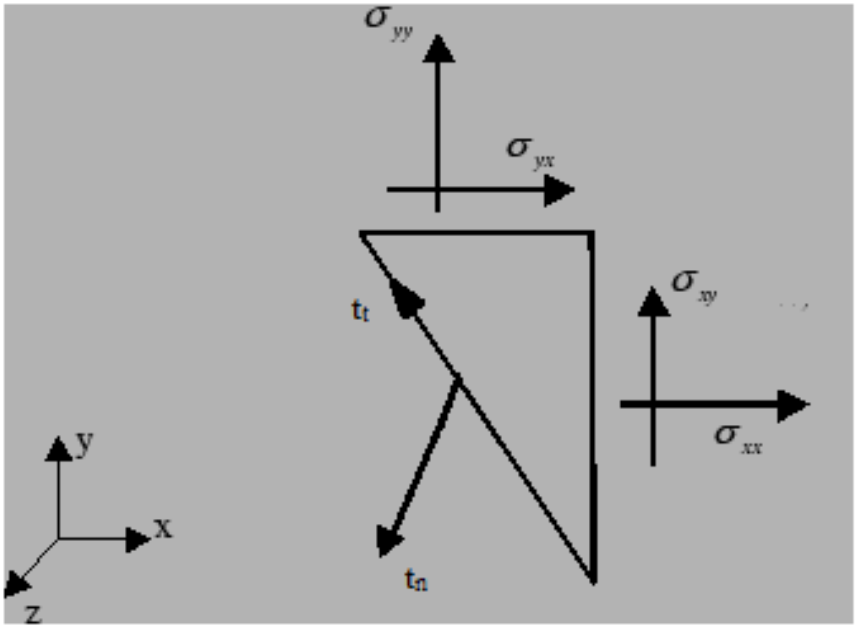

Figure 2: The 2-D free-body diagram with tractions and stress components.

3. RESULTS AND DISCUSSION

Influence of volume fraction on the elastic moduli, E_x, E_y and Gxy are shown figure 3a. The tensile elastic modulus increases with increase of the volume fraction of silicon nitride. Up to 20% of the volume fraction, the compressive elastic modulus increases and for 30% of the volume fraction it decreases. The major Poisson's ratio is increases with increase of the volume fraction of silicon nitride for Si_3N_4/AA5050 alloy metal matrix composites (figure 3b).

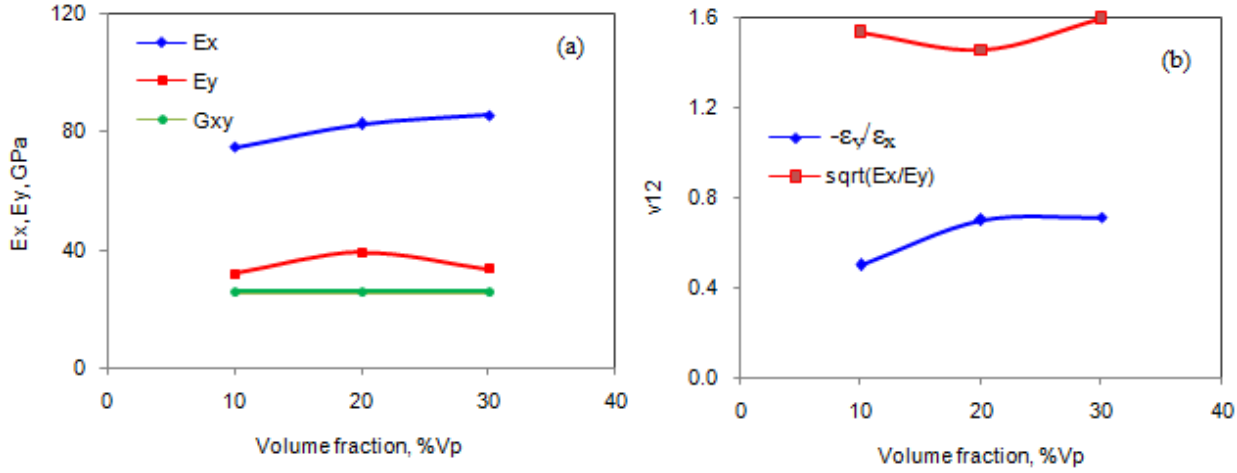

Figure 3: Effect of volume fraction on effective material properties.

The interfacial normal traction, t_n decreases with as θ decreases from 0° to 110° and 190° to 280° (figure 4) and it increases from 110° to 190° and 280° to 360°. The interfacial traction becomes zero at 70°, 130°, 250° and 310° and it reaches maximum

at 0^o, 190^o and 360^o. The normal traction t_n turns into negatively maximum between 70^o and 130^o and again between 250^o and 310^o due to compression of Poisson's effect. The tangential traction t_t, decreases as θ decreases from 0^o to 50^o, from 140^o to 230^o and from 320^o to 360^o. It becomes zero value at $\theta = 100^o$, 190^o and 280^o. The incidence of zero value of normal traction represents the debonding at particle-matrix interface. The incidence of zero value of tangential traction indicates the dislocation. The interfacial normal and tangential displacements are shown in figure 5. The normal and tangential displacements are higher for the low volume fraction of silicon nitride than the high volume fraction. This is owing to the decrease of ductility of the composite with increase of silicon nitride content in the composite.

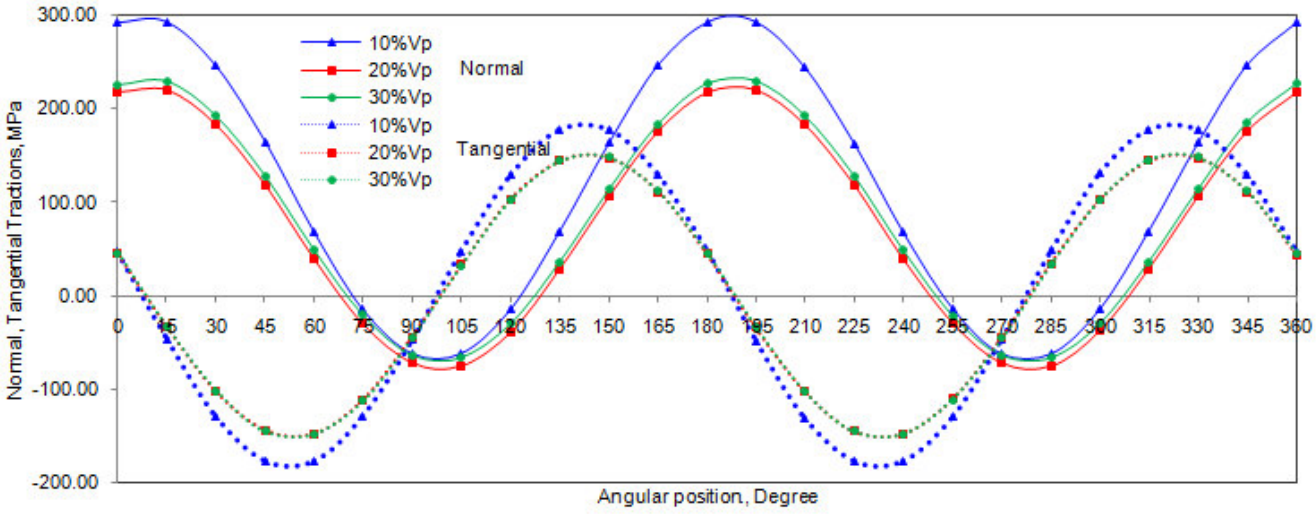

Figure 4: Interfacial tractions due to tensile loading.

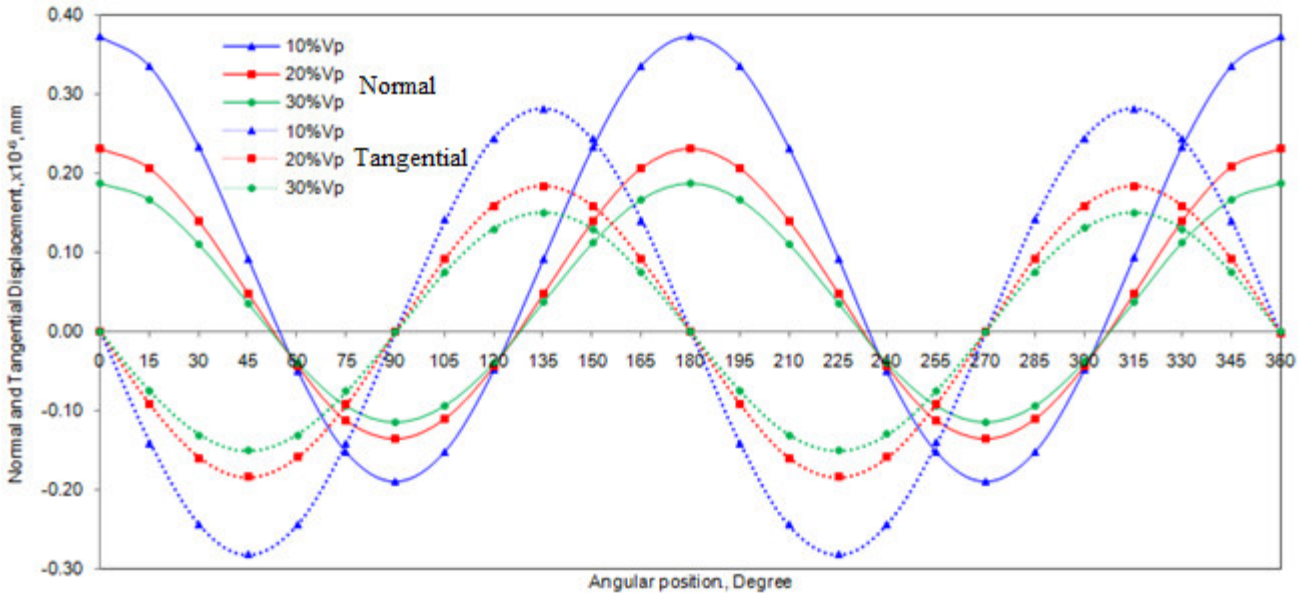

Figure 5: Interfacial displacements due to tensile loading.

The silicon nitride particulate fracture is not occurred as per the condition $\sigma_p < 2\tau/n$ as shown in figure 6a. The particle strength is higher than the interfacial shear stress. The condition for the occurrence of debonding is satisfied as shown in figure 6b. Figure 8 depicts the raster images of results obtained from the finite element analysis. The stress induced in the particle is lower than that induced at the interface between silicon nitride particulate and AA5050 alloy matrix (figure 7a). The shear stress developed at the interface is much higher than that induced in the silicon carbide particulate (figure 7b). This is further confirmed by the von Mises stresses induced in the particle and at the interface (figure 7c). Hence, there is a possibility of debonding at the interface between the particulate and the matrix.

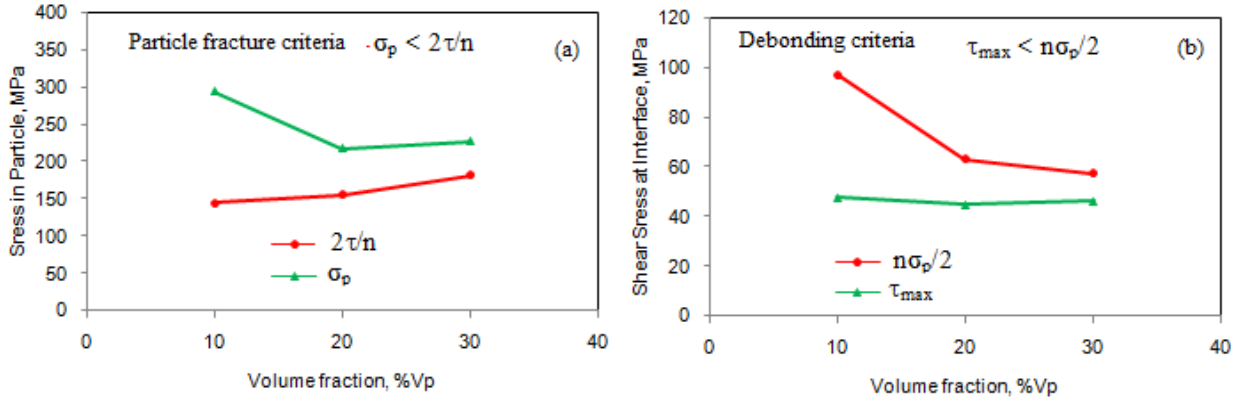

Figure 6: Fracture criteria of: (a) particulate and (b) interface.

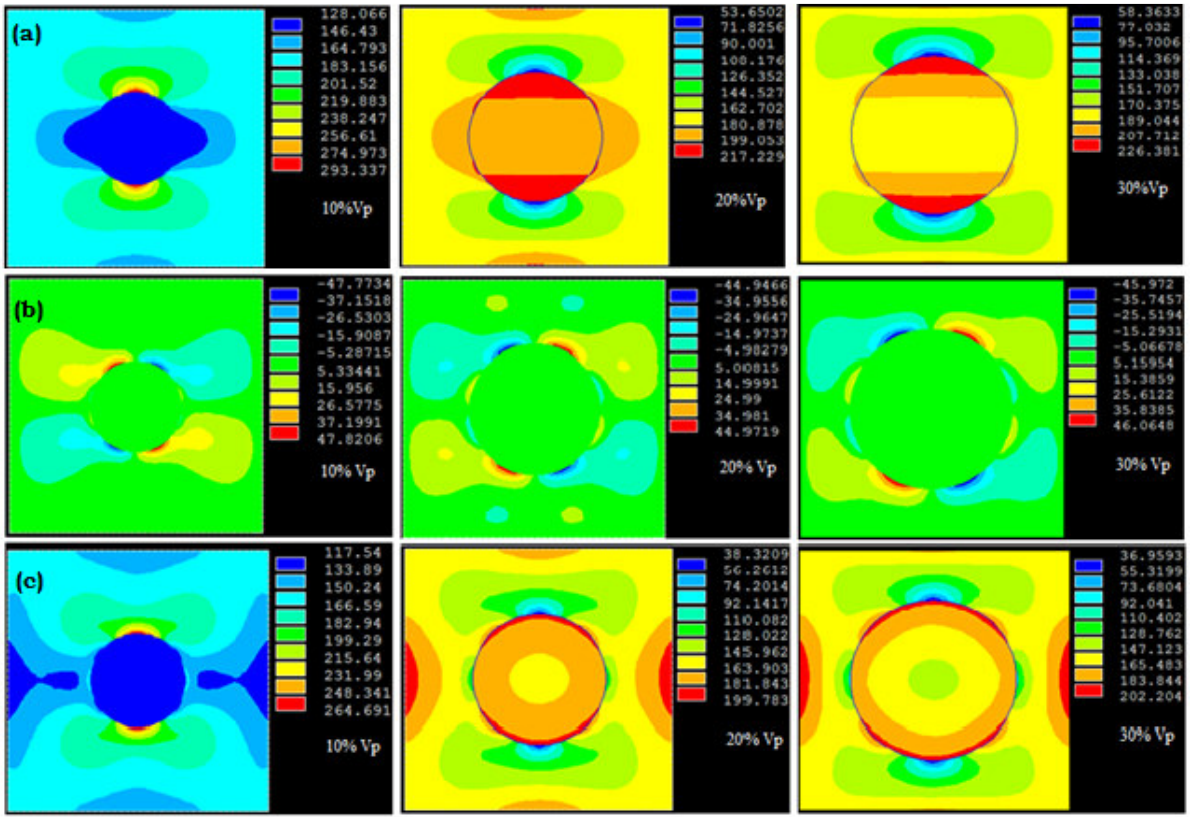

Figure 7: Results obtained from finite element analysis: (a) tensile stress, (b) shear stress and (c) von Mises stress.

4. CONCLUSION

The shear stress induced at the interface between silicon nitride particulate and AA5050 alloy matrix is higher than that induced in the silicon nitride particulate. Therefore, the deboning between particle and matrix take place.

REFERENCES

1. S. Suresh, A. Mortensen, and A. Needleman, Fundamentals of MMCs, Butterworth- Heinemann Publishing Company, Stoneham, USA, 1993.
2. T. S. Srivatsan, Microstructure, tensile properties and fracture behavior of Al_2O_3 particulate-reinforced aluminum alloy metal matrix composites, Journal of Materials Science, vol.31, no.5, 1996, pp.1375-1388.
3. R.J. Arsenault, Relationship between strengthening mechanisms and fracture toughness of discontinuous SiC/Al composites, Journal of Composites Technology, vol.10, 1988, pp.140-145.

4. V.C. Nardone and K.M. Prewo, On the strength of discontinuous silicon carbide reinforced aluminium composites, Scripta Metallurgica, Vol.20, 1986, pp.43-48.
5. H.J. Kim, T. Kobayashi, and H.S. Yoon, Micromechanical fracture process of SiC particulate reinforced Al alloy 6061-T6 MMCs, Materials science and Engineering, Vol.154A, 1992, pp.35-41.
6. D.L. Davidson, Tensile deformation and fracture toughness of 2014 + 15 vol. Pct SiC particulate composite, Metallurgival Transactions, Vol. 22A, 1991, pp.113-123.
7. Y. Flom and R.J. Arsenault, Interfacial bond strength in aluminium alloy 6061-SiC composite, Material Science and Engineering, Vol.77, 1986, pp.191-197.
8. H. L. Cox, The elasticity and strength of paper and other fibrous materials, British Journal of Applied Physics, vol. 3, 1952, pp. 72-79.
9. J. A. Nairn, On the use of shear-lag methods for analysis of stress transfer in unidirectional composites. Mechanics of Materials, vol. 26, 1997, pp. 63-80.
10. S. Sundara Rajan and A. Chennakesava Reddy, Evaluation of Tensile Behavior of Boron Carbide/AA1100 Alloy Metal Matrix Composites, 1st International Conference on Composite Materials and Characterization, Bangalore, March 1997, pp.156-159.
11. P. Martin Jebaraj and A. Chennakesava Reddy, Prediction of Tensile Behavior of Boron Carbide/AA3003 Alloy Metal Matrix Composites, 1st International Conference on Composite Materials and Characterization, Bangalore, March 1997, pp.164-166.
12. A. Chennakesava Reddy, Effect of Particle Loading on Microealstic Behavior and interfacial Tractions of Boron Carbide/AA4015 Alloy Metal Matrix Composites, 1st International Conference on Composite Materials and Characterization, Bangalore, March 1997, pp. 176-179.
13. B. Kotiveera Chari and A. Chennakesava Reddy, Estimation of Micro-stresses and Interfacial Tractions in Boron Carbide/AA5050 Alloy Metal Matrix Composites, 1st International Conference on Composite Materials and Characterization, Bangalore, March 1997, pp. 180-182.
14. H. B. Niranjan and A. Chennakesava Reddy, Valuation of Micro-stresses and interfacial Tractions in Boron Carbide/AA8090 Alloy Metal Matrix Composites, 1st International Conference on Composite Materials and Characterization, Bangalore, March 1997, pp. 189-191.
15. A. Chennakesava Reddy, Interfacial Debonding Analysis in Terms of Interfacial Tractions for Titanium Boride/AA3003 Alloy Metal Matrix Composites, 1st National Conference on Modern Materials and Manufacturing , Pune, 19-20 December, 1997.
16. P. Martin Jebaraj, A. Chennakesava Reddy, Effect of Interfacial Debonding on Stiffness of Titanium Boride/AA5050 Alloy Metal Matrix Composites, 1st National Conference on Modern Materials and Manufacturing , Pune, 19-20 December, 1997.
17. S. Sundara Rajan, A. Chennakesava Reddy, Micromechanical modeling of Titanium Boride/AA7020 Alloy Metal Matrix Composites in Finite Element Analysis using RVE Model, 1st National Conference on Modern Materials and Manufacturing , Pune, 19-20 December, 1997.
18. P. Martin Jebaraj, A. Chennakesava Reddy, Effect of Interfacial Tractions of Rectangular Titanium Boride Particulate/AA8090 Alloy Metal Matrix Composites , 1st National Conference on Modern Materials and Manufacturing , Pune, 19-20 December, 1997.
19. S. Sundara Rajan, A. Chennakesava Reddy, Cohesive Zone interfacial debonding of Silicon Nitride/AA1100 Alloy Metal Matrix Composites Using Finite Element Analysis , 1st National Conference on Modern Materials and Manufacturing , Pune, 19-20 December, 1997.
20. S. Sundara Rajan, A. Chennakesava Reddy, Simulation of Micromechanics for interfacial debonding in Silicon Nitride/AA2024 Alloy Metal Matrix Composites , 1st National Conference on Modern Materials and Manufacturing , Pune, 19-20 December, 1997.
21. P. Martin Jebaraj, A. Chennakesava Reddy, Finite Element Analysis for Assessment of Dislocation and Debonding Events in Silicon Nitride/AA3003 Alloy Metal Matrix Composites, 1st National Conference on Modern Materials and Manufacturing , Pune, 19-20 December, 1997.
22. A. Chennakesava Reddy, Evaluation of Debonding and Dislocation Occurrences in Rhombus Silicon Nitride Particulate/AA4015 Alloy Metal Matrix Composites, 1st National Conference on Modern Materials and Manufacturing , Pune, India, 19-20 December, 278-282, 1997.